Journal of Solid State Chemistry 181 (2008) 2610–2619

Contents lists available at ScienceDirect

Journal of Solid State Chemistry

journal homepage: www.elsevier.com/locate/jssc

Layered double hydroxides as supports for intercalation and sustained release of antihypertensive drugs

Sheng-Jie Xia, Zhe-Ming Ni *, Qian Xu, Bao-Xiang Hu, Jun Hu

College of Chemical Engineering and Materials Science, Zhejiang University of Technology, Hangzhou 310032, PR China

ARTICLE INFO

Article history:
Received 25 March 2008
Received in revised form
23 May 2008
Accepted 2 June 2008
Available online 10 June 2008

Keywords:
Layered double hydroxides
Antihypertensive drugs
Intercalation
Thermal stability
Sustained release

ABSTRACT

Zn/Al layered double hydroxides (LDHs) were intercalated with the anionic antihypertensive drugs Enalpril, Lisinopril, Captopril and Ramipril by using coprecipitation or ion-exchange technique. TG–MS analyses suggested that the thermal stability of Ena^-, Lis^- (arranged with monolayer, resulted from X-ray diffraction (XRD) and Fourier transform infrared spectra (FT-IR) analysis was enhanced much more than Cap^- and Ram^- (arranged with bilayer). The release studies show that the release rate of all samples markedly decreased in both pH 4.25 and 7.45. However, the release time of Ena^-, Lis^- were much longer compared with Cap^-, Ram^- in both pH 4.25 and 7.45, it is possible that the intercalated guests, arranged with monolayer in the interlayer, show lesser repulsive force and strong affinity with the LDH layers. And the release data followed both the Higuchi-square-root law and the first-order equation well. Based on the analysis of batch release, intercalated structural models as well as the TG–DTA results, we conclude that for drug–LDH, stronger the affinity between intercalated anions and the layers is, better the thermal property and the stability to the acid attack of drug–LDH, and the intercalated anions are easier apt to monolayer arrangement within the interlayer, were presented.

1. Introduction

Layered double hydroxides (LDHs), also known as hydrotalcite-like compounds, are a class of host–guest layered solids with the general formula $[M^{2+}_{1-x}M^{3+}_x(OH)_2]^{x+}A^{n-}_{x/n}mH_2O$($M^{2+}$, M^{3+} = di-, trivalent metal cations, A = organic or inorganic anion, m = the number of interlayer water, x = the layer charge density of LDHs) [1]. In recent years, LDHs have received considerable attention because of their application as catalysts, ion exchangers, absorbents, ceramic precursors and organic–inorganic nanocomposites [2–6]. Owing to the intercalation property of LDHs, many LDH compounds with intercalated beneficial organic anions, such as DNA [7], amino acid [8], pesticide [9], plant growth regulators [10] and drugs [11–13] have been prepared. In addition, LDHs is biocompatible and has already found in pharmaceutical applications, such as nonviral vectors for delivery of antisense oligonucleotides [14,15], drug stabilizer [16], a component of anticancer drug in cancer treatment [17], and for the therapy of digestive disorders [18]. Particularly, much attention has been focused on the use of LDHs as support for controlled release formulations of pharmaceuticals such as diclofenac, gemfibrozil, ibuprofen and naproxen, citrate, salicylate and aspartic and glutamic acids has been reported [19–22]. However, very little work has been done to assess the application of LDHs in the preparation of antihypertensive drugs controlled release formulations [23].

In the present work, a series of antihypertensive drugs also known angiotensin-converting enzyme inhibitor including Enalpril, Lisinopril, Captopril and Ramipril, which were widely used to treat hypertensive disease [24–26], were selected as model drugs and intercalated into Zn/Al-NO_3–LDHs successfully by coprecipitation or ion-exchange technique for the first time (except Captopril). We focus on the structure, thermal property and low/controlled release property of as-synthesized drug–LDH composite intended for the possibility of applying these LDH–antihypertensive nanohybrids in drug delivery and controlled release systems.

2. Experimental section

2.1. Materials

All the antihypertensive drugs including Enalpril ($C_{15}H_{21}NO_4$, molecular weight 279, 99.95%, abbreviated as Ena here), Lisinopril ($C_{21}H_{31}N_3O_5$, molecular weight 405, 99.95%, abbreviated as Lis here), Captopril ($C_9H_{15}SNO_3$, molecular weight 217, 99.95%, abbreviated as Cap here), Ramipril ($C_{23}H_{32}N_2O_5$, molecular weight 416, 99.95%, abbreviated as Ram here) were purchased from

* Corresponding author.
E-mail address: jchx@zjut.edu.cn (Z.-M. Ni).

0022-4596/$ - see front matter © 2008 Elsevier Inc. All rights reserved.
doi:10.1016/j.jssc.2008.06.009

Zhejiang Huahai Pharmaceutical Co. Ltd. (China), and used as received. Other inorganic reagents were all of analytical grade (AR) and purchased from Zhejiang Xiaoshan Fine Chemical Co. Ltd. (China) and used without further purification. Deionized water was decarbonated by boiling and bubbling N_2 before employing in all synthesis steps.

2.2. Preparation of samples

2.2.1. Synthesis of nitrate LDHs

Synthesis of LDHs by ion-exchange method was based on the protocol of Miyata [27]. An aqueous solution (100 mL) containing NaOH (24.0 g, 0.6 mol) was added dropwise to a solution (150 mL) containing $Zn(NO_3)_2 \cdot 6H_2O$ (59.4 g, 0.2 mol) and $Al(NO_3)_3 \cdot 9H_2O$ (37.5 g, 0.1 mol) (initial Zn/Al = 2.0) with vigorous stirring until the final pH of 9.5. The resulting slurry was aged at 65 °C for 24 h, and then centrifuged and washed with deionized water until the pH of 7 and was finally dried in vacuo at 85 °C for 18 h, ground and passed through a 100-mesh sieve, giving the product Zn/Al-NO_3–LDHs, denoted as NO_3–LDHs.

2.2.2. Synthesis of Enalpril-NO_3–LDHs by co-precipitation

The Enalpril intercalated nitrate LDHs was prepared by co-precipitation method. An aqueous solution (100 mL) containing NaOH (1.52 g, 0.038 mol) and Ena (3.35 g, 0.012 mol) was added dropwise to a solution (150 mL) containing $Zn(NO_3)_2 \cdot 6H_2O$ (3.56 g, 0.012 mol) and $Al(NO_3)_3 \cdot 9H_2O$ (2.25 g, 0.006 mol) (initial Zn/Al = 2.0) under nitrogen atmosphere with vigorous stirring until the final pH of 9. The resulting slurry was aged at 25 °C for 48 h. Then the resultant was filtered, washed with water until the pH of 7 and finally dried in vacuo at room temperature 48 h. The product was denoted as Ena–LDHs.

2.2.3. Synthesis of Lisinopril-NO_3–LDHs, Captopril-NO_3–LDHs and Ramipril-NO_3–LDHs by ion exchange

The Lisinopril, Captopril and Ramipril intercalated nitrate LDHs were prepared by ion-exchange method. An aqueous solution containing 1.22 g (0.003 mol) of Lisinopril or 0.65 g (0.003 mol) of Captopril or 1.25 g (0.003 mol) of Ramipril in 100 mL of decarbonated water at pH 5 (with 1 M NaOH) was added to 100 mL of an aqueous suspension containing 2.0 g of precursor sample Zn/Al-NO_3–LDHs, respectively. The mixture was magnetically stirred for 3 days at room temperature in nitrogen atmosphere. Then the resultant was filtered, washed with water until the pH of 7 and finally dried in vacuo at room temperature under N_2 atmosphere 48 h. The products were denoted as Lis–LDHs, Cap–LDHs and Ram–LDHs, respectively.

2.3. Characterizations

Powder X-ray diffraction (XRD) patterns were recorded on a Rigaku RINT 2000 powder diffractometer, using Cu$K\alpha$ radiation ($\lambda = 1.54$ Å) at 40 kV and 178 mA and scanning rate of 5°/min in the range of 3–70°.

Fourier transform infrared spectra (FT-IR) were obtained on a Bruker Vector 22 spectrophotometer in the range of 4000–400 cm^{-1} with 2 cm^{-1} resolution by using the standard KBr disk method (sample/KBr = 1/100).

Differential thermal analyses (DTA) and thermogravimetric analyses (TG) were measured on DTA7 and TGA7 instruments, respectively, from Perkin-Elmer. The analyses were carried out in nitrogen atmosphere at a heating rate of 10 °C/min. Simultaneous TG–MS analysis was performed in a Pyris Diamond TG–DTA coupled to ThermoStar^{TM} QM220 mass spectrometer by a quartz capillary transfer line.

Zn and Al element analysis were conducted using inductively coupled plasma (ICP) emission spectroscopy on a Perkin-Elmer Optima 5000DV instrument. Carbon, hydrogen, nitrogen, etc. elemental microanalyses were obtained on an Elementar Vario elemental analyzer.

2.4. Release

The rate of release of the antihypertensive drug anions from the drug–LDHs was determined in a dissolution apparatus with a dissolution paddle assembly. A typical experiment used 1.00 g of powdered drug–LDHs were added in 0.25 dm^3 of buffer solution, using 0.1 mol dm^{-3} HCl solutions or sodium hydrochloride to adjust the initial solutions at pH 4.25 or 7.45. Dispersions were maintained at 37 °C ± 1 for a period of 180 min for pH 4.25, 300 min for pH 7.45, under constant stirring at 100 rpm. At specified time intervals, 2.0×10^{-3} dm^3 of the medium was removed and replaced by an equal volume of fresh receptor solution. The pH values were monitored during every experiment. The amount of released drugs were determined by UV–vis spectrophotometer, using a Hewlett Packard 8453 spectrophotometer, at the wavelength of 235, 255, 205 and 285 nm for Enalpril, Lisinopril, Captopril and Ramipril, respectively.

3. Results and discussion

3.1. Crystal structure and chemical composition of LDH compounds

The XRD diagrams for the samples prepared by co-precipitation or ion exchange are shown in Fig. 1. The XRD patterns exhibit the characteristic reflections of LDHs with a series of (001) peaks, which are sharp and symmetric at low 2θ angle, but broad and asymmetric at high 2θ angle [28]. The original Zn/Al–LDHs collected from the suspension exhibits the typical layered features from XRD patterns (Fig. 1a) and demonstrates a good crystallinity, with 2θ of the 9.986°, (003) spacing of 8.90 Å. The interlayer distance value of d_{003}, representing the summation of thickness of the brucite-like layer (0.48 nm) and the gallery height, which is a function of the number, the size and the orientation of intercalated anions. Successful intercalation of each antihypertensive compound into the LDH host is demonstrated by the XRD diagrams of the nanohybrids (Fig. 2b–e). During ion exchange of

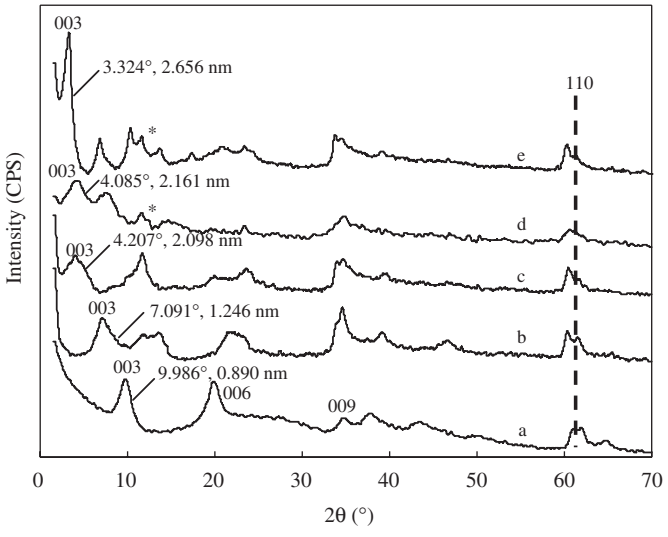

Fig. 1. The XRD patterns of (a) NO_3–LDHs, (b) Ena–LDHs, (c) Lis–LDHs, (d) Cap–LDHs and (e) Ram–LDHs.

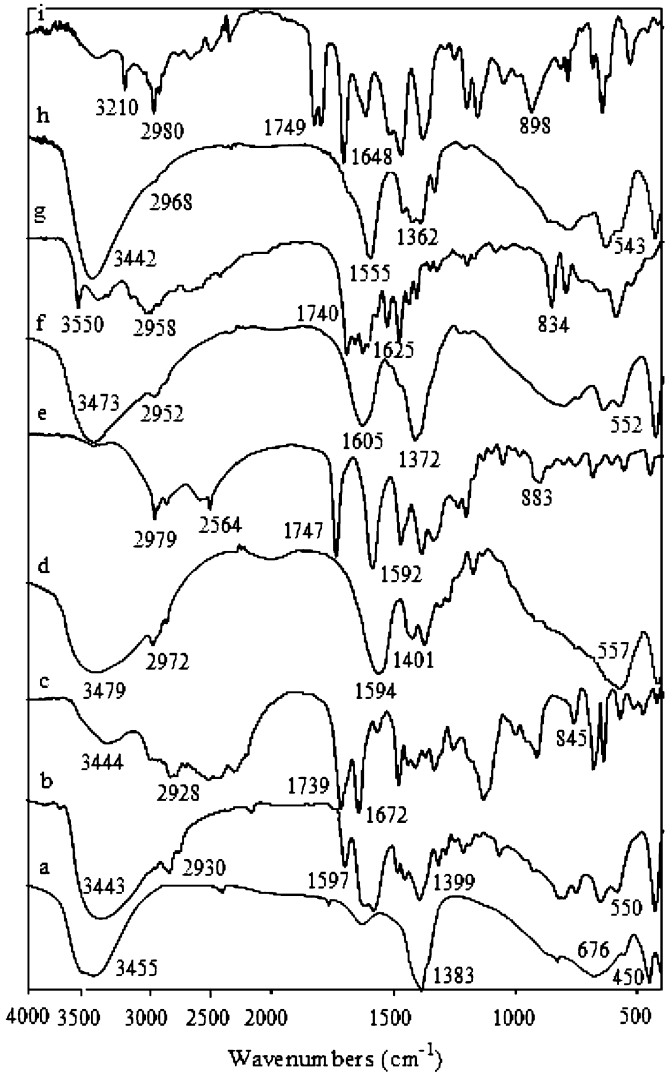

Fig. 2. The IR patterns of samples: (a) NO_3–LDHs, (b) Ram–LDHs, (c) Ram, (d) Cap–LDHs, (e) Cap, (f) Lis–LDHs, (g) Lis, (h) Ena–LDHs and (i) Ena.

the nitrate anions, the layers of LDH expand to host the antihypertensive medical anions and this expansion is reflected by the values of d_{003} which are also given in Fig. 1. These values are 26.56 Å for Ram–LDHs, 21.61 Å for Cap–LDHs, 20.98 Å for Lis–LDHs and 12.46 Å for Ena–LDHs which are larger than those for the Zn/Al–LDHs precursors (8.90 Å), such a swelling of the layers being due to intercalation of the drug molecules. Furthermore, the shoulders at 11.35° 2θ (marked by asterisk) in Fig. 1d, e correspond to the (003) reflection of Zn/Al-CO_3 LDH, while these peaks were overlapped by the (006) reflection in Ena–LDHs (Fig. 1b) and Lis–LDHs (Fig. 1c). This result indicates that there is still some separate Zn/Al-CO_3 LDH phase mixed in the four intercalated materials, although under the protection of nitrogen atmosphere.

The presence of the antihypertensive anions in the nanohybrids can be verified by infrared spectroscopy (IR). Fig. 2 presents the infrared spectra of NO_3–LDHs, antihypertensive drugs and drug–LDHs. For NO_3–LDHs (Fig. 3a), the broad absorption bands at 3455 cm^{-1} arise from the stretching mode of OH groups in the brucite-like layer and physisorbed water; the band at 1383 cm^{-1} due to NO_3^- stretching vibration and the band at 450 cm^{-1} due to O–M–O vibration related to LDHs layers [29]. The FT-IR spectrum of four antihypertensive drugs (Fig. 3c for Ram, Fig. 3e for Cap, Fig. 3g for Lis and Fig. 3i for Ena) in Fig. 3, can be roughly attributed as follows [30]: (1) 3210–3550 cm^{-1} to N–H stretching vibration besides Cap (3444 cm^{-1} for Ram, 3550 cm^{-1} for Lis and 3210 cm^{-1} for Ena); (2) 2928–2980 cm^{-1} to C–H (from COOH group) stretching vibration (2928 cm^{-1} for Ram, 2979 cm^{-1} for Cap, 2958 cm^{-1} for Lis and 2980 cm^{-1} for Ena); (3) 1739–1749 cm^{-1} to the COOH group (1739 cm^{-1} for Ram, 1747 cm^{-1} for Cap, 1740 cm^{-1} for Lis and 1749 cm^{-1} for Ena); (4) 1592–1672 cm^{-1} to C = O vibration (1672 cm^{-1} for Ram, 1592 cm^{-1} for Cap, 1625 cm^{-1} for Lis and 1648 cm^{-1} for Ena) and (5) 834–898 cm^{-1} to CH_2 rocking (845 cm^{-1} for Ram, 883 cm^{-1} for Cap, 834 cm^{-1} for Lis and 898 cm^{-1} for Ena), particularly, for Cap, 2564 cm^{-1} to S–H stretching vibration.

For drug–LDHs (Fig. 3b for Ram–LDHs, Fig. 3d for Cap–LDHs, Fig. 3f for Lis–LDHs and Fig. 3h for Ena–LDHs), indicatives of antihypertensive drugs intercalated in LDHs interlayer space are clearly observed: (1) the bands in the range of 2930–2972 cm^{-1} are attributed to C–H stretching vibration of intercalated antihypertensive anions (2930 cm^{-1} for Ram–LDHs, 2972 cm^{-1} for Cap–LDHs, 2952 cm^{-1} for Lis–LDHs and 2968 cm^{-1} for Ena–LDHs), all quite similar to that of corresponding drugs; (2) the bands at 1739–1749 cm^{-1} due to the COOH group disappears, while the two bands at 1555–1605 cm^{-1} and 1362–1401 cm^{-1} due to the antisymmetric and symmetric stretching vibrations of $-CO_2^-$ appear and shift to lower wavenumbers, compared with free $-CO_2^-$ in antihypertensive drugs, indicating that the intercalation of antihypertensive drugs in the interlayer space involves hydrogen bonding, besides the obvious electrostatic attraction between the electropositive cations in layer and organic anions in interlayer; (3) the bands at 543–557 cm^{-1} are attributed to M–O and M–O–H stretching vibrations of drug–LDHs, which are much smaller than that of NO_3–LDHs (Fig. 3a, 676 cm^{-1}), also confirming the existence of host–guest interaction between the interlayer drug anions and hydroxyl groups of LDH layers, in addition, for Cap–LDHs, the band in 2564 cm^{-1} due to ν(S–H) disappears (Fig. 3d), which is associated with the dissociation of S–H group of Cap at the synthesis pH.

Table 1 lists the chemical compositions of all samples. It should be noted that the determination of chemical compositions of the intercalated materials are due to the results of elemental analysis, TG–DTA analyses (amount of water) and the rule of charge balance as well as the charge on the ion of the interlayer guests. The minimum molecular formulas of all the samples are also given in Table 1, it is clear that the experimental data are in good agreement with the calculated values. Furthermore, small amount of CO_3^{2-} coexist between the layers is probably due to difficulty in completely avoiding contamination from air, which is in consistent with the XRD results. The total exclusion of carbonate from the interlayer space of LDHs is known to be difficult, which can be readily explained on the basis of the favorable lattice stabilization enthalpy associated with the small and highly charged CO_3^{2-} anions [31].

3.2. Thermal stability and supramolecular intercalation structural models

The thermal stability of all samples is investigated by using TG–MS. The TG–DTA profiles are depicted in Figs. 3 and 4 (the MS curves are not given). In the case of pure antihypertensive compounds (Fig. 3a, b and Fig. 4a, b), the DTA curves are quite similar, three main thermal events are clearly observed. The decomposition of the antihypertensive compounds proceeds with turbulence formation, involving processes of vaporization product [32]. The first slow event in the temperature region (90–190 °C) is attributed to the antihypertensive compounds melting, which

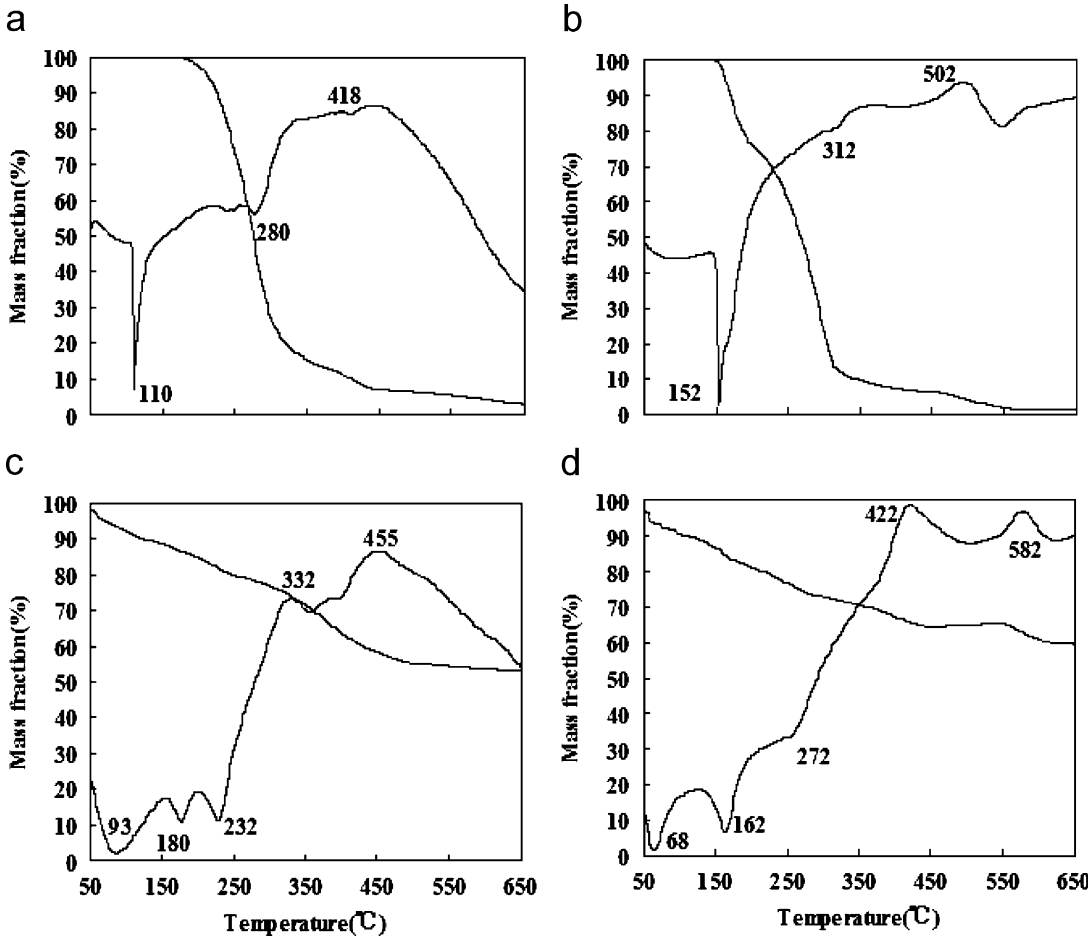

Fig. 3. TG–DTA profiles of (a) Cap, (b) Ena, (c) Cap–LDHs and (d) Ena–LDHs under N_2 atmosphere.

Table 1
Chemical composition of the samples

Samples	Zn%	Al%	S%	C%	H%	N%	O%	Drug%	Chemical formula
NO_3–LDHs	36.99	7.57	–	–	2.72	3.92	48.80	–	$[Zn_{0.67}Al_{0.33}(OH)_2](NO_3^-)_{0.33}\cdot 0.60H_2O$
Ena–LDHs(det)	27.60	5.40	–	23.81	4.69	1.82	36.68	36.12	$[Zn_{0.68}Al_{0.32}(OH)_2](C_{15}H_{20}NO_4^-)_{0.208}(CO_3^{2-})_{0.056}\cdot 0.67H_2O$
Ena–LDHs(cal)	23.04	4.71	–	31.43	5.19	2.44	33.19		$[Zn_{0.67}Al_{0.33}(OH)_2](C_{15}H_{20}NO_4^-)_{0.33}\cdot 0.60H_2O$
Lis–LDHs(det)	30.65	5.99	–	18.48	4.42	3.00	37.46	28.79	$[Zn_{0.68}Al_{0.32}(OH)_2](C_{21}H_{29}N_3O_5^{2-})_{0.103}(CO_3^{2-})_{0.057}\cdot 0.69H_2O$
Lis–LDHs(cal)	26.59	5.44	–	25.39	4.88	4.24	33.46		$[Zn_{0.67}Al_{0.33}(OH)_2](C_{21}H_{29}N_3O_5^{2-})_{0.165}\cdot 0.60H_2O$
Cpl–LDHs(det)	30.02	5.87	4.63	16.07	4.23	2.03	37.15	31.23	$[Zn_{0.68}Al_{0.32}(OH)_2](C_9H_{14}SNO_3^-)_{0.213}(CO_3^{2-})_{0.054}\cdot 0.62H_2O$
Cpl–LDHs(cal)	25.84	5.29	6.26	21.15	4.64	2.74	34.08		$[Zn_{0.67}Al_{0.33}(OH)_2](C_9H_{14}SNO_3^-)_{0.33}\cdot 0.60H_2O$
Ram–LDHs(det)	22.96	4.49	–	31.72	5.24	3.19	32.40	47.22	$[Zn_{0.68}Al_{0.32}(OH)_2](C_{23}H_{31}N_2O_5^-)_{0.219}(CO_3^{2-})_{0.051}\cdot 0.65H_2O$
Ram–LDHs(cal)	18.59	3.81	–	38.89	5.73	3.95	29.03		$[Zn_{0.67}Al_{0.33}(OH)_2](C_{23}H_{31}N_2O_5^-)_{0.33}\cdot 0.60H_2O$

corresponds to a sharp endothermic peak at 110, 152, 105 and 190 °C for Cap, Ena, Lis and Ram, respectively; and the followed stage (200–350 °C) is due to the decomposition and subtle combustion of Cap, Ena, Lis and Ram, which corresponds to a weak endothermic peak at 280 °C for Cap, at 312 °C for Ena, at 280 °C for Lis and at 272 °C for Ram, corresponding to appearance of the *m*/*z* 44 peak (due to CO_2), the *m*/*z* 46 peak (due to NO_2) and 64 peak (due to SO_2 only for Cap) in the MS curves. The last stage (370–550 °C) is due to the strong combustion of Cap, Ena, Lis and Ram, corresponding to a sharp exothermic peak at 418, 502, 530 and 542 °C, the MS curves show several organic signals.

As seen from Fig. 3c, d, the TG–DTA curves of Cap–LDHs and Ena–LDHs reveal five distinguishable weight loss steps, however, it exhibits only four mass loss events for Lis–LDHs and Ram–LDHs according to the DTG curves (see Fig. 4c, d). For Cap–LDHs and Ena–LDHs, the first and second steps in the temperature range 50–180 °C are attributed to the loss of the surface adsorbed and interlayer water, which correspond to two sharp peaks in 93 and 180 °C for Cap–LDHs and in 68 and 162 °C for Ena–LDHs from the DTA profiles, corresponding to the *m*/*z* 18 peak in MS curves. The followed mass loss (200–300 °C) corresponds to a broad DTA effect in 232 °C for Cap–LDHs and 272 °C for Ena–LDHs and is due to the removal of residual intercalated water and trace dehydroxylation of the LDH layer, in this process, the MS curves show also *m*/*z* 18 peak. The fourth mass loss in 300–450 °C corresponds to a broad radiative peak at 332 °C for Cap–LDHs and 422 °C for Ena–LDHs, and is mainly attributed to the dehydroxylation of the LDH layer accompanying with the formation of layered double

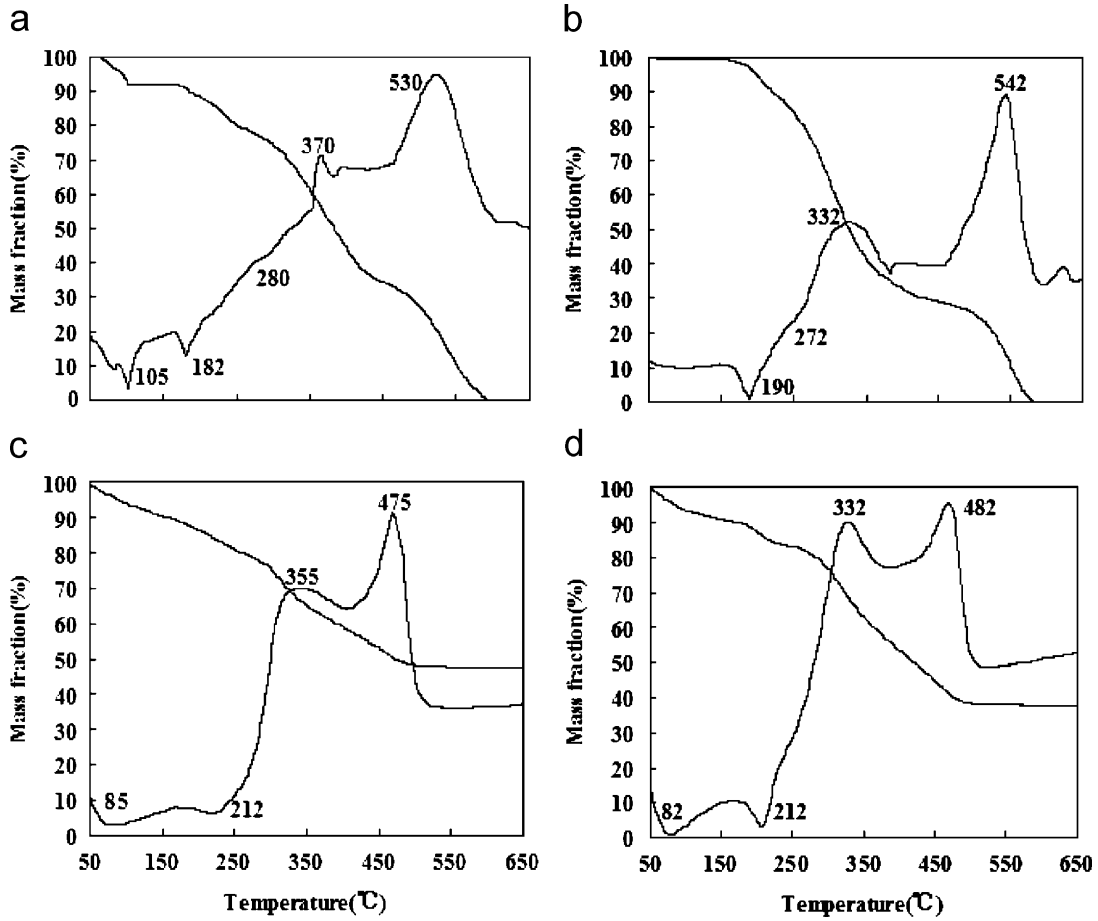

Fig. 4. TG–DTA profiles of (a) Lis, (b) Ram, (c) Lis–LDHs and (d) Ram–LDHs under N_2 atmosphere.

oxide and the partial decomposition/combustion of intercalated Cpl and Ena under N_2 atmosphere, it is fine proved by the MS curves which shows both the *m*/*z* 18 peak (due to H_2O), *m*/*z* 44 peak (due to CO_2), *m*/*z* 46 peak (due to NO_2) and *m*/*z* 64 peak (due to SO_2 only for Cap–LDHs). It should be noticed that this temperature region is obviously higher than that of the pure free Cap and Ena, suggesting that the thermal stability of organic Cap species in Cap–LDHs and Ena species in Ena–LDHs are clearly enhanced due to the host–guest interaction involving the hydrogen bond demonstrated previously by IR analysis. The last mass loss between 450 and 600 °C is the result of further dehydroxylation of the LDHs layers and the complete decomposition of the interlayer guest corresponds to a sharp exothermic peak at ca. 455 °C for Cap–LDHs and 582 °C for Ena–LDHs, Correspondingly, the MS curves show both *m*/*z* 18 peak (due to H_2O) and several organic signals.

For Lis–LDHs and Ram–LDHs, there are only one step in the temperature range 50–150 °C are attributed to the loss of the surface adsorbed and interlayer water; the followed mass loss (180–300 °C) is also due to the dehydroxylation of the LDH layer; the third event (320–450 °C) contains two simultaneous processes: the dehydroxylation of the host matrix and the decomposition of intercalated Lis and Ram, corresponding to a sharp exothermic peak at 355 °C for Lis–LDHs and 332 °C for Ram–LDHs which are higher than original Lis and Ram decomposition temperature. This result also indicates that LDHs host enhances the thermal stability of Lis and Ram; from the analysis of TG–DTA and MS profiles, it is noticeable that the last mass loss in the temperature range 450–550 °C still results from the complete dehydroxylation of the LDH layer and decomposition of intercalated Lis and Ram, but the complete decomposition temperature of Lis and Ram decreases a lot, for Lis, it decline from 530 to 475 °C, and for Ram, from 542 to 482 °C, this result is significantly distinct with other studies before [23,33,34].

According to XRD analysis, the interlayer distance (*d*003) increase to 1.246 nm for Ena–LDHs, 2.098 nm for Lis–LDHs, 2.161 nm for Cap–LDHs and 2.656 nm for Ram–LDHs, and because the value of thickness of the LDH layer is a constant one, which is 0.48 nm [1], thus, the gallery height of LDH after intercalation can be calculated by the interlayer distance minus the thickness of the LDH layer, which are 0.766 nm (1.246–0.48), 1.618 nm (2.098–0.48), 1.681 nm (2.161–0.48) and 2.176 nm (2.656–0.48), respectively. The long axis, short axis and molecular thickness of Ena^-, Lis^-, Cap^- and Ram^- can be calculated from the PM_3 semi-empirical molecular orbital method of Gaussian 03 software, and they are 1.268, 0.763 and 0.492 nm for Ena^-, 1.589, 0.899 and 0.754 nm for Lis^-, 0.839, 0.514 and 0.359 nm for Cap^- and 1.234, 0.960 and 0.711 nm for Ram^-, respectively (see Fig. 5), which are well consisted with other reports [30,35,36].

The gallery height of Ram–LDHs is 2.18 nm, which is far beyond the value of long axis (1.234 nm) and also slight smaller than twice of the long axis dimension (2.468 nm), suggests that the anions are accommodated as alternately tilted bilayer (along the long axis orientation in proper angle) between layers with the carboxyl of adjacent anions attaching to the upper or lower hydroxide layers, respectively. Moreover, the existence of hydrogen bonding interactions between hydroxyl groups and interlayer water molecules may lead to the stability of the composite

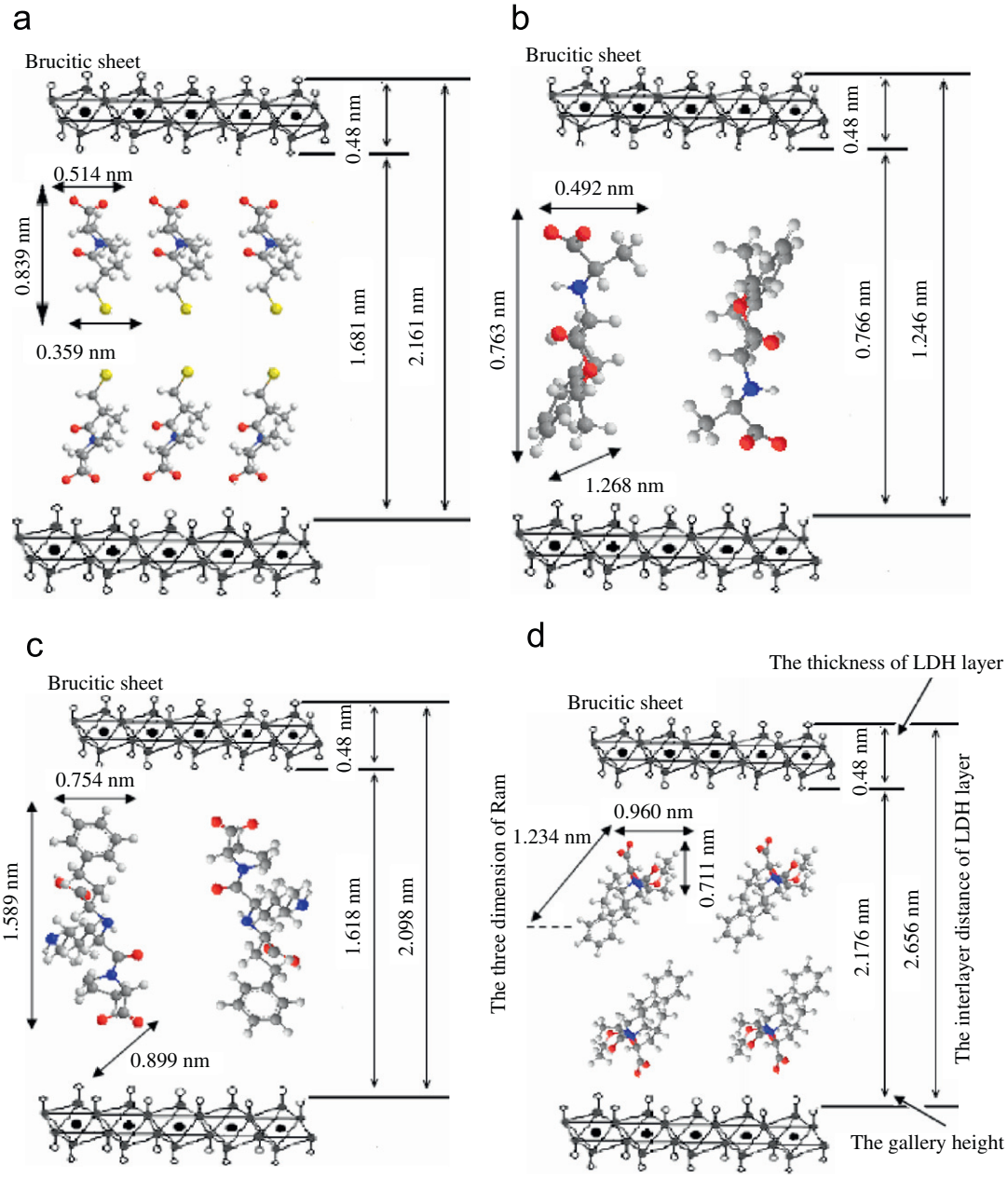

Fig. 5. Schematic illustration of the possible interlayer arrangement and molecular sizes (a) Captopril, (b) Enalpril, (c) Lisinopril and (d) Ramipril.

structure. Comparison of the length of the Cap^- anion (0.839 nm) with the gallery height of Cap–LDHs (1.68 nm) suggests that Cap^- anions are arranged with alternately tilted bilayer (along the long axis orientation) between layers through hydrogen bonding and electrostatic attraction, confirming that the intercalated hydrotalcite has a supramolecular structure. The schematic representation of the probable arrangement for Cap–LDHs and Ram–LDHs is shown in Fig. 5a and d.

While in the case of Ena^- and Lis^-, the value of short axis (0.77 nm) is well consisted with the gallery height of Ena–LDHs (0.783 nm), the value of long axis (1.62 nm) is well consisted with the gallery height of Lis–LDHs (1.599 nm), this indicates that the orientation of guests in LDH interlayer are accommodated as alternately and monolayer vertical (along the short axis for Ena^- and the long axis for Lis^-), and for Ena^-, the negative group of adjacent anions attracted electrostatically to upper or lower hydroxide layers, respectively; for Lis^-, the two negative groups of individual anions attracted electrostatically to upper and lower hydroxide layers, as depicted in Fig. 5b, c. Generally speaking, the two parallel guests which are arranged with bilayer in the interlayer show strong repulsive force, thus, the stability is lower compared with the anions arranged with monolayer. It is well consisted with analysis of TG–DTA, which indicates that the thermal stability enhancement of Ena^-, Lis^- (arranged with monolayer) is much more than Cap^- and Ram^- (arranged with bilayer), this result also proves the rationality of our assumed supramolecular intercalation structure models.

3.3. Sustained release

The curves of release for the Ena^- from Ena–LDH, Lis^- from Lis–LDH, Cap^- from Cap–LDH and Ram^- from Ram–LDH, and the physical mixture (Ena, Lis, Cap and Ram with LDHs) in solutions at pH 4.25 and 7.45 are shown in Fig. 6a and b.

It is obvious that physical mixtures of drugs and LDHs have unconspicuous sustained-release effect both in solutions at pH 4.25 and 7.45. For these mixtures, the total antihypertensive drug content was immediately released, at pH 4.25, in the initial 12 min, release rate of Ena^- from Ena–LDH, Lis^- from Lis–LDH, Cap^- from Cap–LDH and Ram^- from Ram–LDH reached 80.12%, 75.12%, 79.92% and 83.92%, respectively; at pH 7.45, in the initial 17 min, the corresponding values were 83.56%, 78.56%, 83.67% and 83.56, respectively.

Nevertheless, each the antihypertensive drug intercalated LDHs presented a gradual release of the drug anions as a function of time both in solutions at pH 4.25 and 7.45. At pH 4.25 (see Fig. 6a), for these materials, the first aliquot revealed a great amount of the anions (burst effect) [37]. This probably occurs due to the release of the antihypertensive drug anions adsorbed in the LDH surface. Subsequently, with the acid attack, there is a destruction of the layered material and the intercalated antihypertensive drug anions are released. The destruction of the layers increases the pH of the solution due to the release of hydroxyl groups from the layers. In addition, the increase in the pH values causes the decrease of the antihypertensive drug release rate. When the dissolution process of drug–LDH reached the equilibrium state, 81.3% of the Ena^- was released in 92 min and the pH value was 4.78, 76.8% of the Lis^- was released in 92 min and the pH value was 4.97, 80.6% of the Cap^- was released in 62 min and the pH value was 5.15% and 82.8% of the Ram^- was released in 72 min and the pH value was 4.67. The release behavior at pH 7.45 (see Fig. 6b) is also very fast during the first 7 min, which can also be attributed to the release of the antihypertensive drug anions adsorbed in the LDH surface. Subsequently, however, the release of the antihypertensive became much lowers and sustained compared with pH 4.25, with total release occurring up to 232, 232, 172 and 192 min for Ena^-, Lis^-, Cap^- and Ram^-, respectively, after initial exposure, in addition, all the final solution pH were changeless. At and above pH 7, the LDH should be more stable, and as a result, this slow and sustained-release process may be interpreted on the basis of the ion-exchange process between the intercalated anions and chlorine anions in the buffer [10,12]. This hypothesis was confirmed by centrifuging the remaining pH 7.45 drug–LDHs solutions and drying the precipitated host under vacuum overnight. The PXRD pattern of Ena–LDHs was then taken (Fig. 7). The spacing of the peak was at 7.97 Å corresponding to a chloride ion intercalated between the layers of the LDH, consistent with other authors' reports [38–40]. Since chloride is the balancing ion in the buffer, the presence in the layers, and the absence of the Enalpril peak at 12.46 Å shows that it has efficiently replaced all of the Enalpril molecules within the inorganic host. On the basis of the release profiles at pH 4.25 and 7.45, it is found that the equilibrium percentage of Cpl released is not up to 100%. This is probably due to the characteristic of ion-exchange reaction [41,42], i.e. this is an equilibrium process and the interlayer anions cannot be exchanged completely, but the released organic species was removed or consumed continuously.

The proposed equations for release of the antihypertensive drug anions from the drug–LDHs at pH 4.25 (Eq. (1))

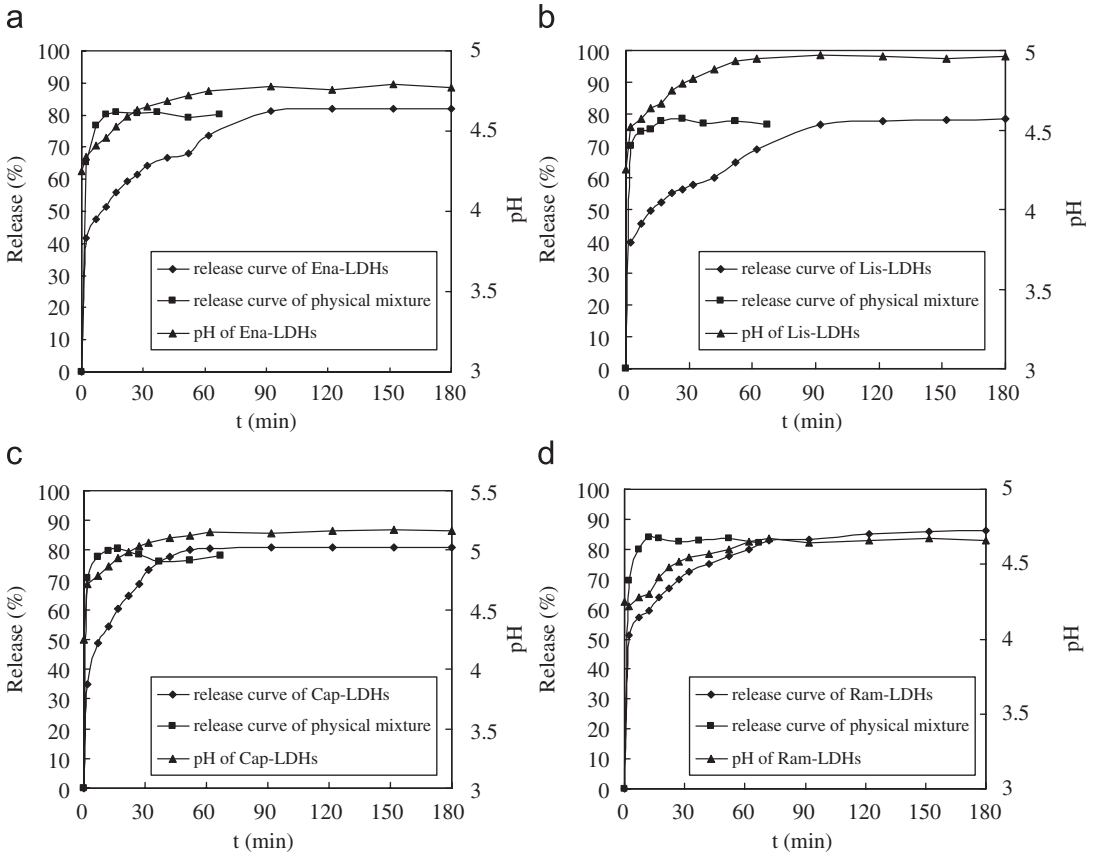

Fig. 6. (a) Release and pH profiles of the antihypertensive drugs: (a) Ena, (b) Lis, (c) Cap and (d) Ram, from the corresponding nanohybrids at pH 4.25. (b) Release and pH profiles of the antihypertensive drugs: (a) Ena, (b) Lis, (c) Cap and (d) Ram, from the corresponding nanohybrids at pH 7.45.

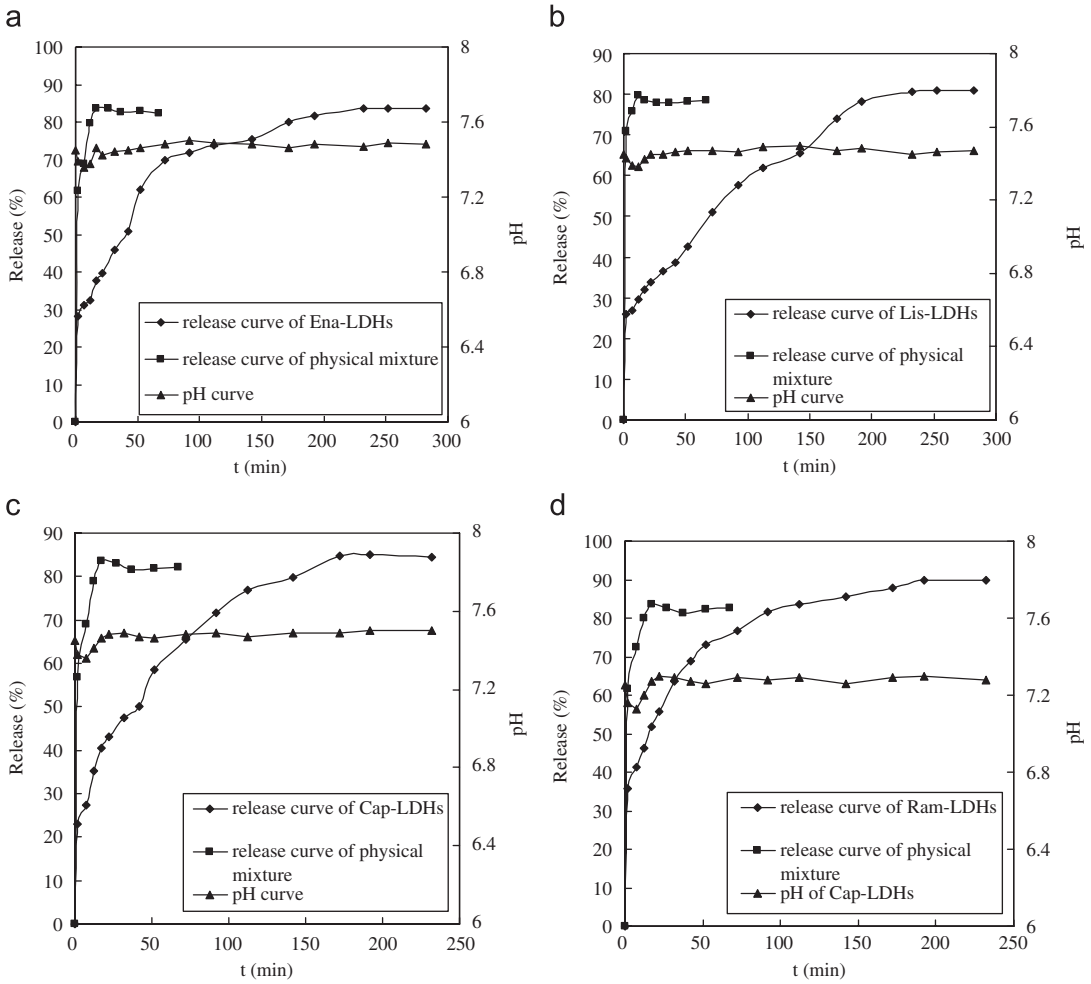

Fig. 6. (*Continued*)

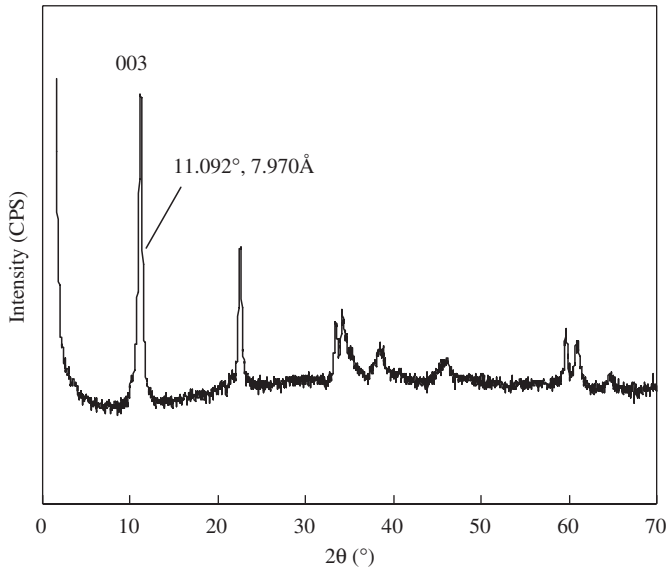

Fig. 7. Powder XRD data for Ena–LDHs released in pH 7.45 solution buffer, centrifuged and dried in vacuum. Peak is at 7.97 Å, corresponding to Cl^- intercalated between the inorganic layers.

and at pH 7.45 (Eq. (2)) are shown below:

$$Mg_xAl_y(OH)_z(Drug)_w nH_2O + mH^+ \rightarrow xMg^{2+} + yAl^{3+} + wH_aDrug^{(3-a)-} + (n+z)H_2O \quad (1)$$

Table 2
Antihypertensive content of the different drug–LDH complexes and total amount of antihypertensive released from the complexes into water during the batch release experiment

Samples	Antihypertensive content % (by chemical formula)	Antihypertensive content % (by release, pH 4.25)	Antihypertensive content % (by release, pH 7.45)
Ena–LDHs	36.12	41.08	42.23
Lis–LDHs	28.79	32.97	34.70
Cap–LDHs	31.23	35.43	37.32
Ram–LDHs	47.22	49.64	53.64

where a depends on the pH (protonation of the drugs), and $m = wa+z$: Every variable can be determined, except the a parameter, that depends on the final pH:

$$Mg_xAl_y(OH)_z(Drug)_w nH_2O + mCl^- \rightarrow Mg_xAl_y(OH)_z(Cl^-)_w nH_2O + (m/a)Drug^{a-} \quad (2)$$

Table 2 shows the content of antihypertensive drugs in the drug–LDH based on the concentration of Ena^-, Lis^-, Cap^- and Ram^- in solutions at the equilibrium state. We can find that the antihypertensive contents released into water are larger than the value measured by chemical formula, this result is consisted with other authors' report [43], and probably due to the portion of the antihypertensive anions adsorbed in the LDH surface, which can also explain the burst release effect during the initial process.

In addition, we also find that the release time of Ena^-, Lis^- which arranged monolayer in LDH interlayer are much longer

Table 3
The fitting results of the drugs release data to different release models at pH 4.25 and 7.45

Samples	First order				Higuchi			
	pH 4.25		pH 7.45		pH 4.25		pH 7.45	
	k_1	R^2	k_1	R^2	k_H	R^2	k_H	R^2
Ena–LDHs	0.0053	0.9775	0.0030	0.9346	4.8177	0.9908	4.5449	0.9646
Lis–LDHs	0.0043	0.9874	0.0027	0.9735	4.3839	0.9926	4.4042	0.9840
Cap–LDHs	0.0102	0.9729	0.0041	0.9674	7.8692	0.9822	5.5168	0.9876
Ram–LDHs	0.0062	0.9815	0.0041	0.9434	4.5084	0.9907	4.4455	0.9781

compared with Cap^-, Ram^- which arranged bilayer, it is possible that the intercalated guests which are arranged with monolayer in the interlayer show lesser repulsive force and strong affinity with the LDH layers, thus, the structure are difficult to destroy compared with the anions arranged with bilayer. Based on this and TG–DTA, we can conclude that LDH Matrices, with higher crystallinity or intercalated with anions of great affinity for the layers, present higher thermal property and more stability to the acid attack and, consequently, have a minor rate of release of the anions.

The kinetic model for the antihypertensive drug anions from the drug–LDHs was analyzed by first-order equation (Eq. (3)) [44] and Higuchi's square root law (Eq. (4)) [45], and the fitting data were given in Table 3:

$$\log(1-X) = -k_1 t \quad (3)$$

$$Q_t = k_H t^{1/2} \quad (4)$$

where X and t are the release percentage and release time, respectively, Q_t the release amount at time t, k_1 and k_H the rate constant of first-order and Higuchi models.

The fitting results are shown in Table 3. The drug anions release from drug–LDHs, presented linear coefficient values (from $\log(1–X)$ vs. t) of 0.9775, 0.9874, 0.9729 and 0.9815 for Ena^-, Lis^-, Cap^- and Ram^- when analyzed by first-order, and the linear coefficient values of 0.9908, 0.9926, 0.9822 and 0.9907, when analyzed by Higuchi model (Q_t vs. $t^{1/2}$) at pH 4.25; and at pH 7.45, the Higuchi model fitting result is also better than fitting by first-order based on corresponding linear coefficients. Therefore, the drug–LDHs follow the Higuchi square root law because the concentration of anion release increased with the square root of time. This way, these results confirmed that the LDHs systems, intercalated with organic anions of pharmaceutical interest, presents a profile of sustained release for the anions.

4. Conclusion

The antihypertensive drugs Enalpril (Ena), Lisinopril (Lis), Captopril (Cap) and Ramipril (Ram) anions pillared Zn-Al LDHs (Zn/Al ratio of 2.03) were successfully assembled by coprecipitation or anion exchange methods. The XRD, FT-IR, UV–vis spectroscopy, TG–DTA and ICP measurements show that the original interlayer nitrate anions of the hydrotalcite can be replaced by antihypertensive anions, obtained drug intercalated Zn-Al LDHs with good crystallinity. In addition, we presume that Ena^- and Lis^- were arranged as monolayer within the interlayer, while Cap^- and Ram^- were bilayer arrangement. And it was found that the interaction of the host layers and the guests is through hydrogen bonding and electrostatic attraction, confirming that the intercalated hydrotalcite has a supramolecular structure. The thermal stability and sustained release of antihypertensive drugs anion-pillared hydrotalcite were enhanced to a considerable extent, comparing with that of antihypertensive drugs. However, the release time of Ena^-, Lis^- were much long compared with Cap^-, Ram^-. The XRD analyses for samples recovered from release media indicate that the dissolution mechanism is mainly responsible for the release behavior of drug–LDHs at pH 4.25, while the ion-exchange one is responsible for that at pH 7.45. Based on analysis of batch release, intercalated structural models and TG–DTA, we conclude that for drug–LDH, stronger the affinity between intercalated anions and the layers is, better the thermal property and the stability to the acid attack of drug–LDH, and the intercalated anions are easier apt to monolayer arrangement within the interlayer, were presented. And the release data followed the Higuchi-square-root law well. Our results indicated the potential applicability of LDHs as supports for the preparation of sustained-release formulations of antihypertensive drugs such as Enalpril, Lisinopril, captopril and Ramipril.

The results reported here demonstrate that Zn/Al-LDO can be used as the effective adsorbent for the removal of methyl orange from aqueous solution.

Acknowledgments

Financial support from the Zhejiang Basic Research Development Program (Grant Y406069) is gratefully acknowledged.

References

[1] F. Cavani, F. Trifir'o, Catal. Today 11 (1991) 173–301.
[2] B. Sels, D.D. Vos, M. Buntinx, F. Pierard, A.K. Mesmaeker, P. Jacobs, Nature 400 (1999) 855–857.
[3] A. Vaccari, Catal. Today 41 (1998) 53–71.
[4] Z.M. Ni, S.J. Xia, L.G. Wang, F.F. Xing, G.X. Pan, J. Colloid Interface Sci. 316 (2007) 284–291.
[5] P.C. Pavan, G.A. Gomes, J.B. Valim, Micropor. Mesopor. Mater. 21 (1998) 659–665.
[6] M. Trikeriotis, D.F. Ghanotakis, Int. J. Pharm. 332 (2007) 176–184.
[7] L. Desigaux, M. Ben Belkacem, P. Richard, J. Cellier, P. Léone, L. Cario, F. Leroux, C. Taviot-Guého, B. Pitard, Nanoletters 6 (2006) 199–204.
[8] Q. Yuan, M. Wei, D.G. Evans, X. Duan, J. Phys. Chem. B 108 (2004) 12381–12387.
[9] G. Lagaly, Appl. Clay Sci. 18 (2001) 205–209.
[10] M.Z. bin Hussein, Z. Zainal, A.H. Yahaya, D.W.V. Foo, J. Control. Rel. 82 (2002) 417–427.
[11] M.D. Arco, E. Cebadera, S. Gutierrez, C. Martin, M.J. Montero, V. Rives, J. Rocha, M.A. Sevilla, J. Pharm. Sci. 93 (2004) 1649–1658.
[12] V. Ambrogi, G. Fardella, G. Grandolini, L. Perioli, M.C. Tiralti, AAPS Pharm. Sci. Technol. 3/3 (2002) article 26.
[13] Z.M. Ni, S.J. Xia, L.G. Wang, F.F. Xing, G.X. Pan, J. Hu, Chem. J. Chin. Univ. 28/7 (2007) 1214–1219.
[14] J.H. Choy, S.Y. Kwak, J.S. Park, Y.J. Jeong, J. Portier, J. Am. Chem. Soc. 121 (1999) 1399–1400.
[15] J.H. Choy, S.Y. Kwak, Y.J. Jeong, J.S. Park, Angew. Chem. Int. Ed. Engl. 39 (2000) 4041–4045.
[16] M. Wei, X.Y. Xu, J. He, G.Y. Rao, H.L. Yang, J. Therm. Anal. Cal. 85 (2006) 795–800.
[17] J.H. Choy, J.M. Oh, M. Park, K.M. Sohn, J.W. Kim, Adv. Mater. 16 (2004) 1181–1184.
[18] Y. Hashimoto, H. Shiozawa, H. Kishimoto, Y. Setoguchi, US Patent, 95307512, 1997, assigned to Rohm and Hass.
[19] M. Del Arco, S. Gutie′rrez, C. Martı′n, V. Rives, J. Rocha, J. Solid State Chem. 177 (2004) 3954–3962.
[20] V. Ambrogi, G. Fardella, G. Grandolini, M. Nocchetti, L. Perioli, J. Pharm. Sci. 92 (2003) 1407–1418.
[21] J. Tronto, E.L. Crepaldi, P.C. Pavan, C.C. de Paula, J.B. Valim, Mol. Cryst. Liq. Cryst. 356 (2001) 227–237.
[22] V. Ambrogi, G. Fardella, G. Grandolini, L. Perioli, Int. J. Pharm. 220 (2001) 23–32.
[23] H. Zhang, K. Zou, S.H. Guo, X. Duan, J. Solid State Chem. 179 (2006) 1792–1801.
[24] S. Takai, D. Yamamoto, D. Jin, S. Inagaki, K. Yoshikawa, K. Tanaka, M. Miyazaki, Eur. J. Pharmacol. 568 (2007) 231–233.
[25] D. Skowasch, A. Viktor, M. Schneider-Schmitt, B. Lüderitz, G. Nickenig, G. Bauriedel, Clin. Res. Cardiol. 95 (2006) 212–216.
[26] G.R. Dagenais, J. Pogue, K. Fox, M.L. Simoons, S. Yusuf, Lancet 368 (2006) 581–588.
[27] S. Miyata, Clays Clay Miner. 28 (1980) 50–56.

[28] Z.P. Xu, H.C. Zeng, J. Phys. Chem. B 105 (2001) 1743–1749.
[29] G. Hu, N. Wang, D. O'Hare, J. Davis, J. Mater. Chem. 17 (2007) 2257–2266.
[30] R. Bhushan, D. Gupta, S.K. Singh, Biomed. Chromatogr. 20 (2006) 217–224.
[31] C.O. Oriakhi, I.V. Farr, M.M. Lerner, J. Mater. Chem. 6 (1996) 103–108.
[32] R.O. Macedo, T. Gomes do Nascimento, C.F. Soares Aragao, A.P. Barreto Gomes, J. Therm. Anal. Cal. 59 (2000) 657–661.
[33] U. Costantino, F. Montanari, M. Nocchetti, F. Canepa, A. Frache, J. Mater. Chem. 17 (2007) 1079–1086.
[34] M. Wei, S.X. Shi, J. Wang, Y. Li, X. Duan, J. Solid State Chem. 177 (2004) 2534–2541.
[35] F.Y. Qu, G.S. Zhu, S.Y. Huang, S.G. Li, J.Y. Sun, D.L. Zhang, S.L. Qiu, Micropor. Mesopor. Mater. 92 (2006) 1–9.
[36] L. Sleno, D.A. Volmer, Rapid Commun. Mass Spectrom. 19 (2005) 1928–1936.
[37] X. Huang, C.S. Brazel, J. Control. Rel. 73 (2001) 121–136.
[38] S. O'leary, D. O'Hare, G. Seeley, Chem. Commun. (2002) 1506–1507.
[39] S. Morlat-Therias, C. Mousty, P. Palvadeu, P. Molinie, P. Leone, J. Rouxel, C. Taviot-Gueho, A. Ennaqui, A.D. Roy, J.P. Besse, J. Solid State Chem. 144 (1999) 143–151.
[40] M.A. Pagano, C. Forano, J.P. Besse, Chem. Commun. (2000) 91–92.
[41] A.M. Fogg, J.S. Dunn, S.G. Shyu, D.R. Cary, D. O'Hare, Chem. Mater. 10 (1998) 351–355.
[42] A.M. Fogg, J.S. Dunn, D. O'Hare, Chem. Mater. 10 (1998) 356–360.
[43] L.P. Cardoso, R. Celis, J. Cornejo, J.B. Valim, J. Agric. Food Chem. 54 (2006) 5968–5975.
[44] N.K. Lazaridis, T.A. Pandi, K.A. Matis, Ind. Eng. Chem. Res. 43 (2004) 2209–2215.
[45] G. Schliecker, C. Schmidt, S. Fuchs, A. Ehingerb, J. Sandowc, T. Kissel, J. Control. Rel. 94 (2004) 25–37.